

## High precision measurement of the radiative capture cross section of $^{238}\text{U}$ at the n\_TOF CERN facility

F. Mingrone<sup>1,2,a</sup>, S. Altstadt<sup>3</sup>, J. Andrzejewski<sup>4</sup>, L. Audouin<sup>5</sup>, V. Bécaries<sup>6</sup>, M. Barbagallo<sup>7</sup>, F. Bečvář<sup>8</sup>, F. Belloni<sup>9</sup>, E. Berthoumieux<sup>9</sup>, J. Billowes<sup>10</sup>, V. Boccone<sup>1</sup>, D. Bosnar<sup>11</sup>, M. Brugger<sup>1</sup>, F. Calviño<sup>12</sup>, M. Calviani<sup>1</sup>, D. Cano-Ott<sup>6</sup>, C. Carrapiço<sup>13</sup>, F. Cerutti<sup>1</sup>, E. Chiaveri<sup>1,9</sup>, M. Chin<sup>1</sup>, N. Colonna<sup>7</sup>, G. Cortés<sup>12</sup>, M.A. Cortés-Giraldo<sup>14</sup>, M. Diakaki<sup>15</sup>, C. Domingo-Pardo<sup>16</sup>, R. Dressler<sup>17</sup>, I. Durán<sup>18</sup>, C. Eleftheriadis<sup>19</sup>, A. Ferrari<sup>1</sup>, K. Fraval<sup>9</sup>, V. Furman<sup>20</sup>, K. Göbel<sup>3</sup>, M.B. Gómez-Hornillos<sup>12</sup>, S. Ganesan<sup>21</sup>, A.R. García<sup>6</sup>, G. Giubrone<sup>16</sup>, I.F. Gonçalves<sup>13</sup>, E. González<sup>6</sup>, A. Goverdovski<sup>22</sup>, E. Griesmayer<sup>23</sup>, C. Guerrero<sup>1</sup>, F. Gunsing<sup>9</sup>, T. Heftrich<sup>3</sup>, A. Hernández-Prieto<sup>1,12</sup>, J. Heyse<sup>24</sup>, D.G. Jenkins<sup>25</sup>, E. Jericha<sup>23</sup>, F. Käppeler<sup>26</sup>, Y. Kadi<sup>1</sup>, D. Karadimos<sup>15</sup>, T. Katabuchi<sup>27</sup>, V. Ketlerov<sup>22</sup>, V. Khryachkov<sup>22</sup>, N. Kivel<sup>17</sup>, P. Koehler<sup>28</sup>, M. Kokkoris<sup>15</sup>, J. Kroll<sup>8</sup>, M. Krtička<sup>8</sup>, C. Lampoudis<sup>9</sup>, C. Langer<sup>3</sup>, E. Leal-Cidoncha<sup>18</sup>, C. Lederer<sup>29</sup>, H. Leeb<sup>23</sup>, L.S. Leong<sup>5</sup>, J. Lerendegui-Marco<sup>14</sup>, R. Losito<sup>1</sup>, A. Mallick<sup>21</sup>, A. Manousos<sup>19</sup>, J. Marganec<sup>4</sup>, T. Martínez<sup>6</sup>, C. Massimi<sup>2,30</sup>, P. Mastinu<sup>31</sup>, M. Mastromarco<sup>7</sup>, E. Mendoza<sup>6</sup>, A. Mengoni<sup>32</sup>, P.M. Milazzo<sup>33</sup>, M. Mirea<sup>34</sup>, W. Mondelaers<sup>24</sup>, C. Paradela<sup>18</sup>, A. Pavlik<sup>29</sup>, J. Perkowski<sup>4</sup>, A.J.M. Plompen<sup>24</sup>, J. Praena<sup>14</sup>, J.M. Quesada<sup>14</sup>, T. Rauscher<sup>35</sup>, R. Reifarh<sup>3</sup>, A. Riego-Perez<sup>12</sup>, M. Robles<sup>18</sup>, C. Rubbia<sup>1</sup>, J.A. Ryan<sup>10</sup>, M. Sabaté-Gilarte<sup>1,14</sup>, R. Sarmiento<sup>13</sup>, A. Saxena<sup>21</sup>, P. Schillebeeckx<sup>24</sup>, S. Schmidt<sup>3</sup>, D. Schumann<sup>17</sup>, P. Sedyshev<sup>20</sup>, G. Tagliente<sup>7</sup>, J.L. Tain<sup>16</sup>, A. Tarifeño-Saldivia<sup>16</sup>, D. Tarrío<sup>18</sup>, L. Tassan-Got<sup>5</sup>, A. Tsinganis<sup>1</sup>, S. Valenta<sup>8</sup>, G. Vannini<sup>2,30</sup>, V. Variale<sup>7</sup>, P. Vaz<sup>13</sup>, A. Ventura<sup>2</sup>, M.J. Vermeulen<sup>25</sup>, V. Vlachoudis<sup>1</sup>, R. Vlastou<sup>15</sup>, A. Wallner<sup>36</sup>, T. Ware<sup>10</sup>, M. Weigand<sup>3</sup>, C. Weiss<sup>23</sup>, T. Wright<sup>10</sup>, P. Žugec<sup>11</sup>, and the n\_TOF Collaboration

- <sup>1</sup> European Organization for Nuclear Research (CERN), Switzerland
- <sup>2</sup> Istituto Nazionale di Fisica Nucleare, Sezione di Bologna, Italy
- <sup>3</sup> Goethe University Frankfurt, Germany
- <sup>4</sup> University of Lodz, Poland
- <sup>5</sup> Institut de Physique Nucléaire, CNRS-IN2P3, Univ. Paris-Sud, Université Paris-Saclay, 91406 Orsay Cedex, France
- <sup>6</sup> Centro de Investigaciones Energéticas Medioambientales y Tecnológicas (CIEMAT), Spain
- <sup>7</sup> Istituto Nazionale di Fisica Nucleare, Sezione di Bari, Italy
- <sup>8</sup> Charles University, Prague, Czech Republic
- <sup>9</sup> CEA Saclay, Irfu, Gif-sur-Yvette, France
- <sup>10</sup> University of Manchester, UK
- <sup>11</sup> University of Zagreb, Croatia
- <sup>12</sup> Universitat Politècnica de Catalunya, Spain
- <sup>13</sup> Instituto Superior Técnico, Lisbon, Portugal
- <sup>14</sup> Universidad de Sevilla, Spain
- <sup>15</sup> National Technical University of Athens, Greece
- <sup>16</sup> Instituto de Física Corpuscular, Universidad de Valencia, Spain
- <sup>17</sup> Paul Scherrer Institut (PSI), Villigen, Switzerland
- <sup>18</sup> University of Santiago de Compostela, Spain
- <sup>19</sup> Aristotle University of Thessaloniki, Thessaloniki, Greece
- <sup>20</sup> Joint Institute for Nuclear Research (JINR), Dubna, Russia
- <sup>21</sup> Bhabha Atomic Research Centre (BARC), India
- <sup>22</sup> Institute of Physics and Power Engineering (IPPE), Obninsk, Russia
- <sup>23</sup> Technische Universität Wien, Austria
- <sup>24</sup> European Commission, Joint Research Centre, Geel, Retieseweg 111, 2440 Geel, Belgium
- <sup>25</sup> University of York, UK
- <sup>26</sup> Karlsruhe Institute of Technology, Campus North, IKP, 76021 Karlsruhe, Germany
- <sup>27</sup> Tokyo Institute of Technology, Japan
- <sup>28</sup> Oak Ridge National Laboratory (ORNL), Oak Ridge, TN 37831, USA
- <sup>29</sup> University of Vienna, Faculty of Physics, Vienna, Austria
- <sup>30</sup> Dipartimento di Fisica e Astronomia, Università di Bologna, Italy
- <sup>31</sup> Istituto Nazionale di Fisica Nucleare, Sezione di Legnaro, Italy
- <sup>32</sup> Agenzia nazionale per le nuove tecnologie (ENEA), Bologna, Italy
- <sup>33</sup> Istituto Nazionale di Fisica Nucleare, Sezione di Trieste, Italy
- <sup>34</sup> Horia Hulubei National Institute of Physics and Nuclear Engineering, Romania

<sup>a</sup>e-mail: federica.mingrone@cern.ch

<sup>35</sup> Department of Physics, University of Basel, Switzerland

<sup>36</sup> Australian National University, Canberra, Australia

**Abstract.** The importance of improving the accuracy on the capture cross-section of  $^{238}\text{U}$  has been addressed by the Nuclear Energy Agency, since its uncertainty significantly affects the uncertainties of key design parameters for both fast and thermal nuclear reactors. Within the 7<sup>th</sup> framework programme ANDES of the European Commission three different measurements have been carried out with the aim of providing the  $^{238}\text{U}(n,\gamma)$  cross-section with an accuracy which varies from 1 to 5%, depending on the energy range. Hereby the final results of the measurement performed at the n\_TOF CERN facility in a wide energy range from 1 eV to 700 keV will be presented.

## 1. Introduction

Nowadays, nuclear energy represents one of a limited number of options available at scale to reduce greenhouse-gas emissions. In this framework, the design of new nuclear reactors rests its foundations upon accurate and precise nuclear data, a list of the most urgent requirements of which has been compiled by the Nuclear Energy Agency [1]. This includes, the measurement of the  $^{238}\text{U}(n,\gamma)$  reaction cross-section because of its key role in the design calculations of nuclear reactors, governing the behaviour of the reactor core. In particular, in the fast region of the neutron spectrum, which is fundamental for the calculation of fast reactors, inconsistencies between published experimental data can reach 15%, and the most recent evaluations disagree with each other. The assessment of nuclear data uncertainties for innovative reactor systems shows that the uncertainty in the radiative capture cross-section of  $^{238}\text{U}$  should be further reduced to 1-3% in the energy region from 20 eV to 25 keV.

To achieve these requirements, within the 7<sup>th</sup> framework programme ANDES of the European Commission three independent measurements have been carried out, two at n\_TOF and one at JRC-Geel [2]. The final results of the  $^{238}\text{U}(n,\gamma)$  measurement performed at the n\_TOF CERN facility will be here presented. It was carried out with a detection system constituted of two liquid scintillators. In the data analysis, special attention was devoted to the identification of all sources of background and to the accurate determination of the various systematic uncertainties.

## 2. Experimental setup

At the neutron time-of-flight facility of CERN, n\_TOF, neutrons are generated in spallation reactions by a pulsed 20 GeV/c proton beam impinging on a lead block. The neutron source is surrounded by 4 cm of water plus 1 cm of borated water, which serves as a coolant and as a moderator of the originally fast neutron spectrum [3]. The resulting white neutron beam ranges from thermal energies up to 1 GeV. The neutrons travel through a vacuum beam line to the experimental area, located at the nominal distance of 185 m from the spallation target. This very long flight path provides an excellent energy resolution, allowing to resolve closely spaced neutron resonances.

The experimental technique used for this measurement is the Total Energy technique, which requires that the efficiency of the detection system is directly proportional to the total radiative energy emitted by the capture event. To achieve this proportionality a low solid angle detection system has been used, consisting in two  $\text{C}_6\text{D}_6$  liquid

scintillators, one commercial BICRON and one custom made (*Forschungszentrums Karlsruhe*—FZK) [4], placed face to face at 90° with respect to the neutron beam direction. Afterwards, the response of the detector has been weighted applying the so-called weighting function, which has been calculated by means of the pulse-height weighting technique [5].

The  $^{238}\text{U}$  sample used is an extremely pure metallic plate, approximately rectangular in shape, with an area of  $1621.2 \pm 0.1 \text{ mm}^2$  and a mass of  $6.125 \pm 0.002 \text{ g}$ . In order to cover the same fraction of the neutron beam, the other samples measured for background evaluation have been prepared with the same geometry.

## 3. Data reduction

During the measurement, the stability has been checked both for the neutron flux and for the scintillators, and runs that showed a deviation in the counting rate of more than 3.5% have been rejected. An accurate study of the calibrations between the flash-ADC channels and the energy deposited by the  $\gamma$ -rays in the detectors has been performed on a weekly basis.

To calculate the weighting functions (WF) required by the total energy detection technique, the detector responses have been simulated with the GEANT4 toolkit [7] and convoluted with the experimental resolution. Two WF have been produced: one considering an homogenous emission of the  $\gamma$ -rays, used for the analysis of both the resolved and unresolved resonance region, the other considering an exponential attenuation along the neutron beam direction to take into account the effects of neutron transport within the sample, not negligible in the saturated resonances that are exploited to extract the normalization factor.

The capture yield is the observable quantity measured in a capture reaction, and it is related to the weighted counting rate  $C$  by [6]:

$$Y_{exp}(E_n) = N \frac{C(E_n) - B(E_n)}{A\varepsilon\phi_n(E_n)}, \quad (1)$$

where  $B(E_n)$  indicates the contribution of the background,  $\varepsilon$  the efficiency of the detection system,  $A$  the effective area of the sample intercepted by neutron beam and  $\phi_n$  the incident neutron flux. To compare the experimental yield to its expected value, the geometry of the whole system (including the effective area of the sample) and the absolute value of the neutron fluence are included into a single and energy-independent normalization factor  $N$ .

To reach the aimed precision for the cross section, a very accurate and precise characterization of the background that affects the measurements is fundamental.

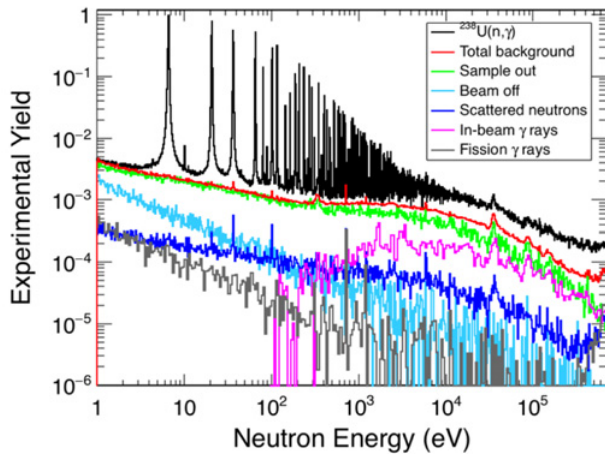


**Figure 1.**  $^{238}\text{U}(n,\gamma)$  capture yield compared with the total background and its individual components discussed in the text. The yields have been obtained separately for each one of the two detectors and summed afterwards.

Five different contributions have been identified and characterized both through experimental measurement and MonteCarlo simulations. In Fig. 1 these component are shown with respect to the  $^{238}\text{U}$  capture yield. The time independent component of the background, due to the natural and sample radioactivity and to air activation, have been evaluated in a beam-off measurement. The background related only to the neutron beam has been measured without any sample in-beam to take into account all the sources of background in the experimental area. Three background components have been associated to the presence of the sample in-beam: first of all, the background due to  $\gamma$ -rays coming from sample-scattered neutrons captured in the environmental material (the so-called neutron sensitivity). Although the detectors exploited for this measurement have been optimized to minimize this kind of background, its contribution cannot be neglected since it follows the same energy dependence as the true capture events and may therefore compromise the analysis of the resonances. To properly evaluate it, GEANT4 simulations have been performed with a complete description of the geometry of the experimental area [8]. Secondly, we evaluated the background contribution due to in-beam  $\gamma$ -rays through a  $n+^{208}\text{Pb}$  measurement, properly scaled to take into account the differences in areal density and charge number between the uranium and lead samples. The third sample-related background component comes from the  $\gamma$ -rays emitted in both fission events and decays of fission fragments. This has been evaluated by means of a complete set of GEANT4 simulations describing the experimental area and the sample.

To validate the background level, it has been additionally evaluated with an independent method exploiting the presence of Ag, W, Co and Al black-resonance filters in beam. The resulting background has been properly scaled to take into account the attenuation of both the neutron beam and the in-beam photons. The two background yields agree for  $3 < E_n < 100$  keV within 5% except near the big Al resonances, because the total amount of aluminum in the windows of the beam line is not precisely known.

The neutron flux for the n\_TOF facility has been evaluated combining together the results of five different

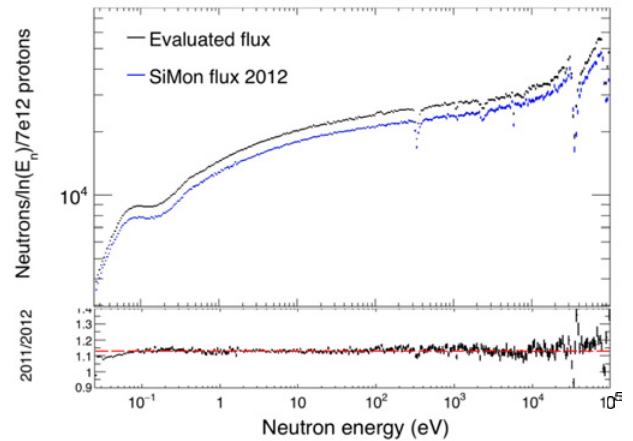


**Figure 2.** n\_TOF neutron flux in 2012 (blue) compared with the 2011 evaluated flux. The ratio is plotted in the bottom panel.

**Table 1.** The three different normalization factors obtained from the saturated resonances for the two  $\text{C}_6\text{D}_6$  scintillators.

Detector	$N_1$	$N_2$	$N_3$
Bicron	0.842	0.843	0.850
FZK	1.008	0.995	1.001

detectors, as described in Ref. [9]. For the 2012 measurement campaigns not all detectors were available. However during the entire measurement the flux at the sample position was controlled by a thin  $^6\text{Li}$  foil that is placed in beam and viewed by a silicon detector [10]. As can be seen in Fig. 2, the absolute value of the flux is 13% lower in 2012 with respect to the evaluated flux, unless a loss of efficiency occurred, possibly due to a change of the position of the SiMON detector or to a degeneration of the  $^6\text{Li}$  converter foil. Nevertheless, above 0.1 eV the flux remains constant in shape within 2% (bottom panel of Fig. 2). This constant behaviour allows to use the evaluated flux to extract the yield for the  $^{238}\text{U}(n,\gamma)$  measurement from 0.1 eV neutron energy, providing that the difference in intensity is taken into account in the normalization procedure.

The  $^{238}\text{U}$  sample has been chosen in such a way that the first three resonances ( $E_n = 6.67, 20.9$  and  $36.7$  eV, respectively) are saturated, and therefore the normalization factor  $N$  can be extracted by applying the saturated resonance method. The expected capture yield has been evaluated through a least-squares adjustment of the experimental data with the SAMMY code [11]. The two detectors have been treated separately, and in Table 1 the different results are shown. The final normalization factors have been chosen as the average of the three resonances, and the mean deviation of these factors of 1% has been adopted as the normalization uncertainty.

## 4. Results

The Resolved Resonance Region (RRR) in this work is limited up to 3 keV by the decrease of the signal-to-background ratio with neutron energy together with the limited counting statistics. Within this energy range a resonance shape analysis of the s-wave resonances has been performed by means of the multilevel multichannel

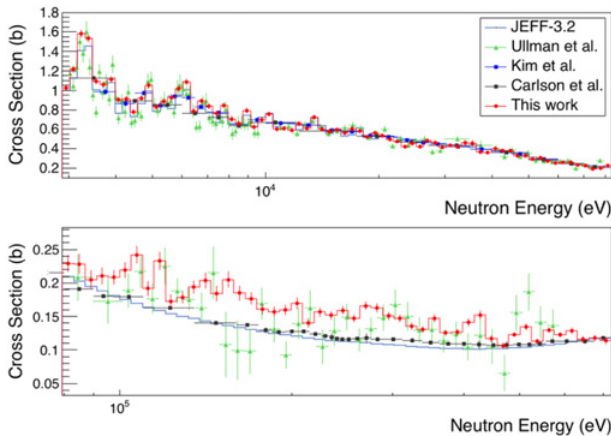


**Figure 3.**  $^{238}\text{U}(n,\gamma)$  cross section from this work compared to previous measurements by Ullman et al. [13] and Kim et al. [14], and with the cross-section recommended by Carlson et al. [15]. The top panel shows neutron energies from 3 to 80 keV, while the bottom panel from 80 to 700 keV. The evaluated cross sections from JEFF-3.2 is plotted for comparison.

R-matrix code SAMMY [11], starting from the parameters reported in the JEFF-3.2 evaluated library [12]. The resonance kernels (defined as  $\kappa = g\Gamma_n\Gamma_\gamma/(\Gamma_n + \Gamma_\gamma)$ ) have been used in the comparison with evaluated libraries. In particular, the statistical distribution of kernel ratios of this work over JEFF-3.2 and this work over ENDF/B-VII.1 is gaussian peaked at 0.99 and 1.00 respectively, with a sigma of 0.06, illustrating the good agreement between this work and the evaluated libraries.

For energies from 3 to 700 keV, the capture cross-section is obtained by applying to the experimental yield a correction factor that takes into account the sample-related effects, i.e. self-shielding and multiple scattering followed by capture. In this Unresolved Resonance Region (top panel of Fig. 3) from 3 to 80 keV data from this work are in good agreement with previous measurements by Ullman et al. [13] and Kim et al. [14], with the cross-section recommended by Carlson et al. [15], and with the JEFF-3.2 evaluated cross-section. In the high energy region from 80 to 700 keV, the cross-section from this work deviates by more than a 20% from both the cross-section recommended by Carlson et al. and from the JEFF-3.2 evaluated cross-section, while it is still in fair agreement with the cross section obtained by Ullman et al. [13].

## 5. Conclusions

The radiative capture cross-section of  $^{238}\text{U}$  has been measured at the n\_TOF facility of CERN in the wide energy range from 1 eV up to 700 keV.

The very careful data reduction, with particular emphasis on the background evaluation and subtraction, has allowed to extract the experimental yield with very low correlated uncertainties.

The resonance shape analysis has been performed up to 3 keV, showing in general fair agreement with the evaluated libraries. In the URR results from this work are in fair agreement with previous measurements and evaluated libraries up to 80 keV, but are about 20% higher from 80 to 700 keV.

## References

- [1] NEA Nucler Data High Priority Request List, <http://www.nea.fr/html/dbdata/hpr1/>
- [2] P. Schillebeeckx et al., *Total and radiative capture cross section measurements for  $^{238}\text{U}$  at GELINA and n\_TOF* (European Commission, 2013)
- [3] C. Guerrero et al., *The European Physical Journal A* **49**, 49 (2013)
- [4] R. Plag et al., *Nucl. Instr. Methods Phys. Res. A* **496**, 425 (2003)
- [5] A. Borella et al., *Nucl. Instr. Methods Phys. Res. A* **577**, 626 (2007)
- [6] P. Schillebeeckx et al., *Nuclear Data Sheets* **113**, 3054 (2012)
- [7] S. Agostinelli, J. Allison, K. Amako et al., *Nucl. Instr. Methods Phys. Res. A* **506**, 250 (2003)
- [8] P. Žugec et al., *Nucl. Instr. Methods Phys. Res. A* **760**, 57 (2014)
- [9] M. Barbagallo et al., *Eur. Phys. J. A* **49**, 156 (2013)
- [10] S. Marrone et al., *Nucl. Instr. Methods Phys. Res. A* **517**, 389 (2004)
- [11] N.M. Larson, ORNL/TM-9179/R8, ENDF-364/R2 (Oak Ridge National Laboratory, 2008)
- [12] A.J. Koning et al., *Journal of the Korean Physical Society* **2**, 1057 (2011)
- [13] J.L. Ullmann et al., *Phys. Rev. C* **89**, 034603 (2014)
- [14] H.I. Kim et al., *Eur. Phys. J. A* **52**, 170 (2016)
- [15] A.D. Carlson et al., *Nucl. Data Sheets* **110**, 3215 (2009)